

# Bose-Einstein condensation of exciton polaron-polaritons

Aleksi Julku,<sup>1</sup> Miguel. A. Bastarrachea-Magnani,<sup>1,2</sup> Arturo Camacho-Guardian,<sup>3</sup> and Georg Bruun<sup>1,4</sup>

<sup>1</sup>*Center for Complex Quantum Systems, Department of Physics and*

*Astronomy, Aarhus University, Ny Munkegade, DK-8000 Aarhus C, Denmark*

<sup>2</sup>*Departamento de Física, Universidad Autónoma Metropolitana-Iztapalapa, San Rafael Atlixco 186, C.P. 09340 CDMX, Mexico*

<sup>3</sup>*T.C.M. Group, Cavendish Laboratory, University of Cambridge, JJ Thomson Avenue, Cambridge, CB3 0HE, U.K*

<sup>4</sup>*Shenzhen Institute for Quantum Science and Engineering and Department of Physics, Southern University of Science and Technology, Shenzhen 518055, China*

(Dated: February 11, 2022)

Exciton polaritons in two-dimensional semiconductors inside microcavities are powerful platforms to explore hybrid light-matter quantum systems. Here, we study the Bose-Einstein condensation of polaron-polaritons, which are quasiparticles formed by the dressing of exciton polaritons by particle-hole excitations in a surrounding electron gas. Using a non-perturbative many-body theory to describe exciton-electron correlations combined with a non-equilibrium theory for the condensate, we show that the electrons strongly affect the condensate. This stems from the dependence of the polaron-polariton energy and the interaction between them on the electron density, which leads to highly nonlinear effects. We identify stable and unstable regimes of the condensate by calculating its excitation spectrum, and show that they result in prominent hysteresis effects when the electron density is varied. Our results should be readily observable using present experimental technology.

Exciton-polaritons featuring a coherent superposition of light and matter have gained widespread attention for exhibiting several interesting effects such as non-equilibrium Bose-Einstein condensation [1, 2], superfluidity [3, 4], quantum vortices [5], and topological photonics [6–9]. Recently, systems comprising exciton-polaritons interacting with an electron gas in microcavity semiconductors, such as monolayer transition metal dichalcogenides (TMDCs), have been explored both theoretically and experimentally [10–14]. An exciting perspective of these hybrid light-matter systems is the realisation of strong optical nonlinearities [13, 14] with applications in optoelectronics [15, 16].

When an electron gas is injected into a semiconductor, it can interact with the excitons to form exciton polarons [17, 18]. Coupling to cavity photons in turn makes them into polaron-polaritons [10, 13, 14, 19]. While focus so far has mostly been on the limit of low polariton density, these systems can realise other interesting regimes of physics as well. Depending on the ratio between the polariton and electron densities, this includes a gas of trions, i.e. bound-states of excitons and electrons [20–24], electrons dressed by polaritons forming electron polaron-polaritons, and Bose-Fermi mixtures [25], see Fig. 1. Indeed, experiments realising atomic Bose-Fermi mixtures have shown that they exhibit rich physics such as mediated interactions [26], phase separation [27], mixed superfluids [28], and the breakdown of the Fermi polaron [29]. It is therefore interesting to explore such mixtures in the hybrid light-matter setting of polaritons, which offer new possibilities for probing and control.

Motivated by this, we investigate here the case where the polariton density is large enough to create a Bose-Einstein condensate (BEC) immersed in an electron gas. Combining a many-body theory for polaron-polaritons

with a Bogoliubov theory for the non-equilibrium BEC created by a pump laser, we show that the condensate properties are dramatically affected by the electrons. This is because both the energy and the effective interaction between the polaron-polaritons depend on the electron density, which therefore serves as a new experimental knob. In particular, we demonstrate that one can drive the condensate into stable and unstable regimes with very different densities resulting in prominent hysteresis effects as shown in Fig. 1(b)-(c). The arrow in Fig. 1(a) illustrates our approach, which extends the previously studied polaron-polaritons in an electron gas into the regime of Bose-Fermi mixtures.

*System.*— We study polaritons created in a two-dimensional semiconductor in a microcavity pump-probe experiment where the excitons strongly couple to the cavity light field. In addition, they interact with each other as well as with an electron gas (2DEG). The excitons are treated as a point bosons due to their binding energy, which is typically much larger than any other relevant energy scale in semiconductors such as the TMDCs [16, 30]. The Hamiltonian is

$$H = \sum_{\mathbf{k}} [\hat{x}_{\mathbf{k}}^{\dagger} \quad \hat{c}_{\mathbf{k}}^{\dagger}] \begin{bmatrix} \epsilon_{x\mathbf{k}} & \Omega \\ \Omega & \epsilon_{c\mathbf{k}} \end{bmatrix} \begin{bmatrix} \hat{x}_{\mathbf{k}} \\ \hat{c}_{\mathbf{k}} \end{bmatrix} + \sum_{\mathbf{k}} \epsilon_{e\mathbf{k}} \hat{e}_{\mathbf{k}}^{\dagger} \hat{e}_{\mathbf{k}} + \sum_{\mathbf{k}, \mathbf{k}', \mathbf{q}} \left( g_{ex} \hat{x}_{\mathbf{k}'-\mathbf{q}}^{\dagger} \hat{e}_{\mathbf{k}+\mathbf{q}}^{\dagger} \hat{e}_{\mathbf{k}} \hat{x}_{\mathbf{k}'} + \frac{g_{xx}}{2} \hat{x}_{\mathbf{k}'-\mathbf{q}}^{\dagger} \hat{x}_{\mathbf{k}+\mathbf{q}}^{\dagger} \hat{x}_{\mathbf{k}} \hat{x}_{\mathbf{k}'} \right), \quad (1)$$

where  $\hat{x}_{\mathbf{k}}$ ,  $\hat{c}_{\mathbf{k}}$  and  $\hat{e}_{\mathbf{k}}$  are the annihilation operators for an exciton, cavity photon and electron, respectively, with energies  $\epsilon_{x\mathbf{k}} = \mathbf{k}^2/2m_x$ ,  $\epsilon_{c\mathbf{k}} = \mathbf{k}^2/2m_c + \delta$  and  $\epsilon_{e\mathbf{k}} = \mathbf{k}^2/2m_e$ , and masses  $m_x$ ,  $m_c$ , and  $m_e$ . The exciton-photon coupling strength is  $\Omega$ , and the electron-exciton  $g_{ex}$  and exciton-exciton  $g_{xx}$  interactions are taken to be momentum independent due to their short range nature. We use units where the system area and  $\hbar$  are one, and

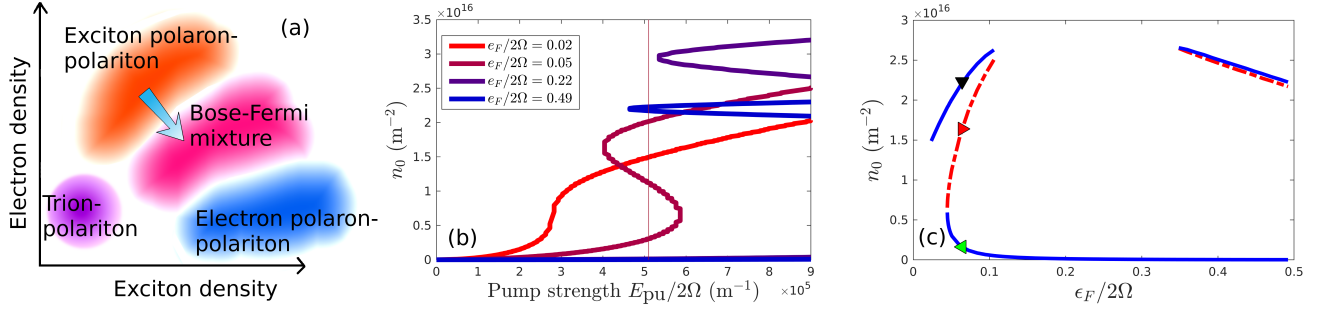


FIG. 1. (a) Schematic diagram illustrating the different physical regimes realised by polaron-polaritons in a 2DEG. The arrow represents our approach to analyse the Bose-Fermi mixture, using the polaron-polaritons as our starting point. (b) Condensate density  $n_0$  as a function of pump laser amplitude  $E_{\text{pu}}$  for the pump frequency  $\epsilon_{\text{pu}}/2\Omega = -2.22$  and various electron densities. (c) Condensate density as a function of electron density for fixed pump laser amplitude indicated by the vertical line in (b). Blue/red lines indicate stable/unstable configurations.

the energy offset of the electrons relative to the excitons is absorbed in their chemical potential  $\mu_e$ . In the absence of interactions, diagonalization of Eq. (1) yields the energies  $\epsilon_{\mathbf{k}}^{LP/UP} = \frac{1}{2}(\epsilon_{c\mathbf{k}} + \epsilon_{x\mathbf{k}} \pm \sqrt{\tilde{\delta}_{\mathbf{k}}^2 + 4\Omega^2})$  of the lower (LP) and upper (UP) polariton [31]. They are depicted in Fig. 2(a) as black lines for  $\mathbf{k} = 0$  as a function of the detuning  $\delta$ .

*Polaron-polaritons.*— The interaction between the excitons and electrons in the presence of strong light coupling has been observed to lead to the formation of polaron-polaritons [10, 13, 14], in analogy with the realisation of Fermi polarons in atomic gases [32]. A convenient way to describe them is to introduce a  $2 \times 2$  matrix Green's function, which in Matsubara frequency space reads [12, 33]

$$G(\mathbf{k}, i\omega_n) = \begin{bmatrix} i\omega_n - \epsilon_{x\mathbf{k}} - \Sigma_x(\mathbf{k}, i\omega_n) & -\Omega \\ -\Omega & i\omega_n - \epsilon_{c\mathbf{k}} \end{bmatrix}^{-1} \quad (2)$$

where the effects of the strong exciton-electron interaction are included via the exciton self-energy

$$\Sigma_x(\mathbf{k}, i\omega_n) = \int \frac{d^2\mathbf{q}}{4\pi^2} n_F(\epsilon_{e\mathbf{q}} - \mu_e) \mathcal{T}(\mathbf{k} + \mathbf{q}, i\omega_n + \epsilon_{e\mathbf{q}} - \mu_e). \quad (3)$$

Here,  $\omega_n$  is a bosonic Matsubara frequency and  $n_F(x) = (\exp \beta x + 1)^{-1}$  is the Fermi-Dirac distribution function. Here,  $\mathcal{T}(\mathbf{k}, i\omega_n)$  is the exciton-electron scattering matrix  $\mathcal{T}(\mathbf{k}, i\omega_n)$ , which in the ladder approximation reads  $\mathcal{T}^{-1}(\mathbf{k}, i\omega_n) = \text{Re}\Pi_V(\epsilon_B) - \Pi(\mathbf{k}, i\omega_n)$  with  $\Pi$  and  $\Pi_V$  being the exciton-electron pair propagator in the presence of the 2DEG and in a vacuum, respectively [33–36]. The exciton-electron interaction is strong enough to support a bound state, the trion, giving rise to a pole of the scattering matrix at its energy, which is shifted away from its vacuum value  $\epsilon_B$  due to medium effects.

We plot in Fig. 2(a) the photon spectral function  $A_c(\mathbf{k}, \omega) = -2\text{Im}[G_c(\mathbf{k}, \omega + i0^+)]$  for zero momentum  $\mathbf{k} = 0$ . Here, and in the rest of the paper, we take

$m_x = 2m_e$ ,  $m_c = 10^{-5}m_e$ , and use an experimentally inspired value for the trion energy  $\epsilon_B/2\Omega = -1.56$  [10, 13, 37] with  $\Omega = 8$  meV. The electron density is set to  $n_e = 1.58 \times 10^{16} \text{ m}^{-2}$  corresponding to the Fermi energy  $\epsilon_F/2\Omega = 0.46$ . Furthermore,  $\mu_e = \epsilon_F$  as we focus on the zero-temperature limit. Figure 2(a) exhibits three quasiparticle branches obtained by solving in its diagonal basis  $\text{Re}[G^{-1}(\mathbf{k}, \epsilon_{\mathbf{k}})] = 0$  giving

$$\epsilon_{\mathbf{k}}^{L/U} = \frac{1}{2} \left[ \epsilon_{c\mathbf{k}} + \epsilon_{x\mathbf{k}} + \Sigma_x(\mathbf{k}, \epsilon_{\mathbf{k}}^{L/U}) \pm \sqrt{\tilde{\delta}_{\mathbf{k}}^2 + 4\Omega^2} \right]. \quad (4)$$

Here,  $\tilde{\delta}_{\mathbf{k}} = \epsilon_{c\mathbf{k}} - \epsilon_{x\mathbf{k}} - \Sigma_x(\mathbf{k}, \epsilon_{\mathbf{k}}^{L/U})$  and  $L/U$  labels the lower/upper polariton branch. Depending on the values of  $\delta$  and  $\epsilon_F$ , either  $\epsilon_{\mathbf{k}}^U$  or  $\epsilon_{\mathbf{k}}^L$  has two solutions giving rise to the three polaron-polariton branches in Fig. 2(a), which differ significantly from the bare polariton branches.

From now on, we focus on the lowest energy  $\mathbf{k} = 0$  polaron-polariton for  $\delta/2\Omega = -2.11$  indicated by the red star in Fig. 2(a). In Fig. 2(b), we plot its energy  $\epsilon_{\mathbf{k}=0}^L \equiv \epsilon_0$  as a function of the electron density parametrised by  $\epsilon_F$ . We see that it decreases with increasing  $\epsilon_F$  as it gets increasingly repelled by the trion state.

*Polaron-polariton interaction.*— The effective interaction  $g$  between zero-momentum polaron-polaritons, responsible for the non-linear optical properties, is modified by the coupling to the 2DEG. It is given by

$$g = g_{xx} \tilde{C}^4(\mathbf{k} = 0) Z^2(\mathbf{k} = 0) \quad (5)$$

where  $\tilde{C}(\mathbf{k}) = 1/2(1 + \tilde{\delta}_{\mathbf{k}}/\sqrt{\tilde{\delta}_{\mathbf{k}}^2 + 4\Omega^2})$  is the generalised Hopfield coefficient, which takes into account that polaron-polaritons interact only via their excitonic component. Compared to the usual Hopfield coefficients [31], it includes many-body effects via the detuning  $\tilde{\delta}_{\mathbf{k}}$ . The quasiparticle residue  $Z^{-1}(\mathbf{k}) = 1 - \tilde{C}^2(\mathbf{k})\partial_{\omega} \Sigma_x(\mathbf{k}, \omega)|_{\epsilon_0}$  describes the fact that many-body correlations reduce the plane wave component of the polaron-polariton as compared to the bare polaritons and is typical for microscopic

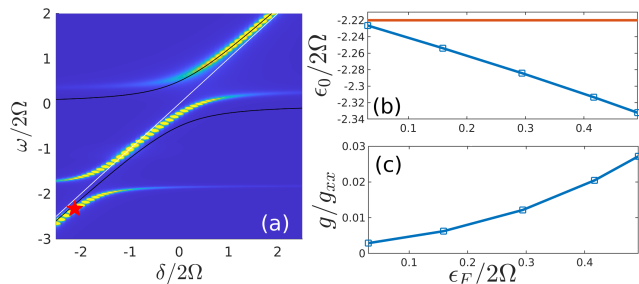


FIG. 2. (a) Spectral density of a single cavity photon. White line is the bare photon energy and black lines are the bare upper and lower polariton dispersions. The energy  $\epsilon_0$  of the lowest polaron-polariton branch at  $\delta/2\Omega = -2.11$  is indicated by a red star (b) The energy  $\epsilon_0$  as a function of the electron density. The pump frequency at  $\epsilon_{\text{pu}}/2\Omega = -2.22$  is shown as a horizontal line. (c) The interaction between two polaron-polaritons as a function of the electron density.

expressions of effective interactions between quasiparticles [38, 39].

We focus on the regime where the energy  $\epsilon_0$  of the lowest polaron-polariton is well below that of the trion. It follows that exchange interactions mediated by the electrons or the trions can be safely neglected [12].

To analyse the effects of the 2DEG on the interaction between the polaron-polaritons, we plot in Fig. 2(c)  $g$  as a function of  $\epsilon_F$ . This shows that the interaction increases significantly with the electron density. The reason is that the electrons decrease the polaron-polariton energy, Fig. 2(b), which increases  $\tilde{\delta}_{\mathbf{k}}$  and therefore the excitonic component of the polaron-polaritons given by  $\tilde{C}(\mathbf{k})$ . The two effects shown in Fig. 2, the decrease in the polaron-polariton energy and the increase in their interaction, play a key role for the non-linear effects we present later.

Determining the value of the bare exciton-exciton interaction strength  $g_{xx}$  remains a challenging problem, and there are several discrepancies between theory and experiment. While it has been estimated that  $g_{xx} \sim \mathcal{O}(10)\mu\text{eV}\mu\text{m}^2$  in GaAs quantum wells [40–43], theoretical calculations predict  $g_{xx} \sim 2\mu\text{eV}\mu\text{m}^2$  in TMDCs [44] whereas experimental estimates range from  $g_{xx} \sim 0.05\mu\text{eV}\mu\text{m}^2$  [13, 45] to  $g_{xx} \sim 3.0\mu\text{eV}\mu\text{m}^2$  [14]. In this work we choose  $g_{xx} = 3\mu\text{eV}\mu\text{m}^2$ . Using a smaller interaction would yield larger condensation densities without changing the results qualitatively.

We note that the single particle properties of polaron-polaritons are remarkably well described with an equilibrium theory such as the one employed here [10]. Contrary to this, it is known that the driven-dissipative nature of semiconductor microcavity systems gives rise to qualitatively new effects for polariton BECs [46–48]. Consequently, we will employ a non-equilibrium theory to describe the behaviour of the polaron-polariton BECs.

*Condensation of polaron-polaritons.*— We are now

ready to analyse the properties of polaron-polariton BECs in the presence of a 2DEG. The system is assumed to be driven coherently by a continuous pump laser with zero angle incidence, which introduces a macroscopic occupation to the  $\mathbf{k} = 0$  ground state of the polaron-polaritons with energy  $\epsilon_0$ , marked by the red star in Fig. 2(a). Due to its pump-loss nature, the resulting BEC is described by a non-equilibrium Gross-Pitaevskii equation (GPE) of the form [33, 46–48]

$$[\epsilon_{\text{pu}} - \epsilon_0(\epsilon_F) - g(\epsilon_F)|\Psi|^2 + i\gamma]\Psi = iE_{\text{pu}}. \quad (6)$$

Here,  $\Psi$  is the condensate wave function,  $\epsilon_{\text{pu}}$  is the pump laser frequency, and  $E_{\text{pu}}$  is its amplitude. We use an experimentally realistic value  $\gamma = 0.4$  meV for the polaron-polariton loss rate due to processes such as exciton decay and photon leakage through the cavity mirrors [14]. Note that in Eq. (6) we have explicitly expressed the dependence of  $\epsilon_0$  and  $g$  on  $\epsilon_F$  to highlight that these are the parameters being varied when the electron density is tuned as shown in Fig. 2. The pump laser frequency is  $\epsilon_{\text{pu}}/2\Omega = -2.22$  as indicated by the horizontal line in Fig. 2(b), which shows that the laser becomes increasingly blue detuned with respect to the polaron-polaritons as the electron density gets larger.

In Fig. 1(b), we plot the condensate density  $n_0 = |\Psi|^2$  obtained from Eq. (6) as a function of the pump laser amplitude  $E_{\text{pu}}$  for different electron densities. We see that as the electron density increases, an s-shape feature emerges, which is characteristic of hysteresis effects. The height of the s-shape first increases and then decreases with  $\epsilon_F$ . This non-trivial behavior is due to the combination of an increasing blue detuning of the laser and the growth of the interaction strength with the increase of the electron density.

To further investigate how the electrons affect the BEC, we plot in Fig. 1(c) the condensate density as a function of the electron density for a fixed pump laser amplitude indicated by the vertical line in Fig. 1(b). This shows that the s-shaped curves in Fig. 1(b) yield three solutions for low and high electron densities. The behavior for low density  $\epsilon_F$  arises predominantly due to the increasing blue detuning of the laser with increasing electron density. This is similar to what can be observed when the laser frequency  $\epsilon_{\text{pu}}$  is tuned for polariton BECs without the 2DEG [46–48]. The behavior for large electron density, on the other hand, arises due to an intricate interplay between an increasing blue detuning and an increasing coupling strength [33]. Consequently, it is a unique property of the Bose-Fermi mixture, which cannot be observed without the 2DEG.

*Excitation spectrum.*— To explore the stability of the solutions of the GPE, we calculate the excitation spectrum of the BEC of polaron-polaritons. As shown in the Supplemental material [33], Bogoliubov theory generalised to the non-equilibrium pump-loss setup yields

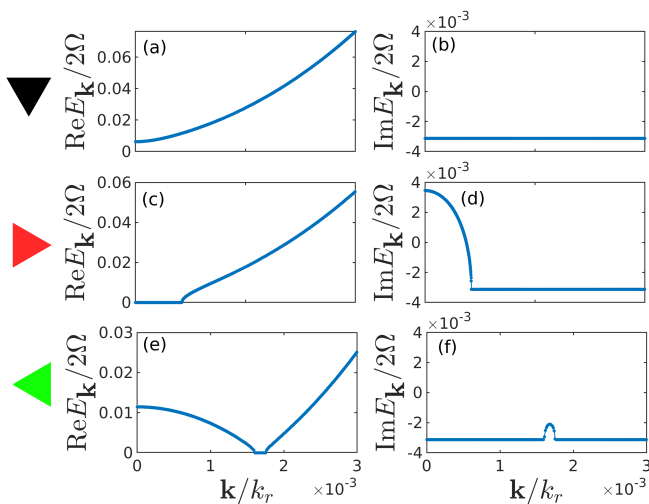


FIG. 3. Bogoliubov dispersions  $E_{\mathbf{k}}$  as a function of the in-plane momentum  $\mathbf{k}$  for the three different cases marked by the triangles in Fig. 1(c). Panels (a), (c) and (e) show  $\text{Re}[E_{\mathbf{k}}]$  and panels (b), (d) and (f) show  $\text{Im}[E_{\mathbf{k}}]$ . Momenta are expressed in the units of  $k_r = \sqrt{4\pi n_0}$ . The stability of different cases can be deduced from the sign of the imaginary part of  $E_{\mathbf{k}}$ .

the  $2 \times 2$  boson Green's function

$$G_B^{-1}(\mathbf{k}, \omega) = \begin{bmatrix} \omega - \tilde{\epsilon}_{\mathbf{k}} + i\gamma - 2gn_0 & -gn_0 \\ -gn_0 & -\omega - \tilde{\epsilon}_{\mathbf{k}} - i\gamma - 2gn_0 \end{bmatrix}, \quad (7)$$

where  $\tilde{\epsilon}_{\mathbf{k}} = \epsilon_{\mathbf{k}}^L - \epsilon_{\text{pu}}$ , with  $\epsilon_{\mathbf{k}}^L$  being the energy of the lower polaron-polariton as a function of momentum  $\mathbf{k}$  obtained from solving Eq. (4). Note that the single-particle energy in the hole-channel is conjugated since it contains the decay  $\gamma$  [33]. The excitation energies  $E_{\mathbf{k}}$  can then be found as the poles of  $G_B(\mathbf{k}, \omega)$ , giving

$$E_{\mathbf{k}} = \sqrt{(\tilde{\epsilon}_{\mathbf{k}} + 2gn_0)^2 - (gn_0)^2} - i\gamma. \quad (8)$$

We plot in Fig. 3 the excitation spectrum  $E_{\mathbf{k}}$  for the three cases marked by the coloured triangles in Fig. 1(c). The top panels show the case marked by the black triangle in Fig. 1(c) corresponding to  $\epsilon_F/2\Omega = 0.064$  and  $n_0 = 2.2 \times 10^{16} \text{ m}^{-2}$ . We see that the spectrum is gapped, which is because the pump laser breaks the  $U(1)$  phase symmetry of the wave function  $\Psi$  explicitly in contrast to the gapless Goldstone mode of equilibrium BECs [47, 48]. Moreover, the energies have a negative imaginary part for all  $\mathbf{k}$ , meaning that the condensate is stable.

Figs. 3(c)-(d) depict the case marked by the red triangle in Fig. 1(c) with  $\epsilon_F/2\Omega = 0.064$  and  $n_0 = 1.64 \times 10^{16} \text{ m}^{-2}$ . The real part of  $E_{\mathbf{k}}$  is exactly zero and the imaginary part is positive for small momenta. This feature emerges when the square root in Eq. (8) becomes negative for  $-3gn_0 < \tilde{\epsilon}_{\mathbf{k}} < -gn_0$ , giving a purely imaginary contribution to the energy. For small  $k$ , this is larger than the loss rate  $\gamma$  making the system dynamically unstable.

Finally, the spectrum shown in Figs. 3(e)-(f) is for the case marked by the green triangle in Fig. 1(c) with  $\epsilon_F/2\Omega = 0.064$  and  $n_0 = 1.63 \times 10^{15} \text{ m}^{-2}$ . Here, the spectrum is qualitatively different with a low momentum regime exhibiting an inverted parabolic shape. As a consequence, there is a range of  $k$ -values where the modes are gapless, above which the energy again increases. The effect of the 2DEG is, however, not large enough to render the system unstable.

By analysing the stability of all the solutions of the GPE shown in Fig. 1(c), we can identify the stable and unstable regions of the BEC, which are marked by blue/red lines respectively. These stable/unstable regions give rise to an interesting hysteresis behaviour of the condensate and demonstrate that different regimes of the Bose-Fermi mixture can be reached by tuning the electron density.

*Outlook and conclusions.*— We have explored the non-equilibrium condensation of polaron-polaritons in the presence of a 2DEG. Using a non-perturbative many-body theory, we first showed that the electrons affect both the energy of the polaron-polaritons and the interaction between them. The interplay of these two effects were then demonstrated to lead to a highly non-linear behaviour of the condensate, which was analysed using a non-equilibrium Bogoliubov theory. In particular, the condensate can be in stable and unstable regimes with very different densities resulting in prominent hysteresis effects depending on the electron density.

Polaritons have already been observed to exhibit non-linear behavior when the pump laser frequency is varied [49, 50], and one has furthermore realised polaron-polaritons in the presence of a 2DEG [10, 20, 51]. Thus, the interesting effects presented here for the polaron-polariton condensate should be within reach of present day experimental technology by combining such experiments. From a broader perspective, our results demonstrate that polaritons immersed in an electron gas can realise novel hybrid light-matter Bose-Fermi mixtures with interesting properties. This motivates future investigations into such mixtures where optical non-linearities have been observed [13, 14] and strong mediated interactions between the polaron-polaritons predicted [12, 52]. Inspired by atomic gases, one may observe phase separation [27], strong coupling effects [53, 54], boson mediated topological and exotic superfluidity [55, 56]. Our theoretical approach is based on the polaron picture, which for Fermi polarons in atomic gases have been shown to be accurate for surprisingly high polaron densities [57]. It is an interesting challenge to develop a theory that accounts for strong coupling effects both on the polaritons and on the electrons, while describing the non-equilibrium condensation in a systematic way.

G.M.B. acknowledges financial support from DNRf through the Center for Complex Quantum Systems (Grant agreement No. DNRf156) and the Independent

Research Fund Denmark-Natural Sciences (Grant No. DFF-8021-00233B). A.J. acknowledges financial support from the Jenny and Antti Wihuri Foundation.

- 
- [1] J. Kasprzak, M. Richard, S. Kundermann, A. Baas, P. Jeambrun, J. M. J. Keeling, F. M. Marchetti, M. H. Szymańska, R. André, J. L. Staehli, V. Savona, P. B. Littlewood, B. Deveaud, and L. S. Dang, *Nature* **443**, 409 (2006).
- [2] H. Deng, H. Haug, and Y. Yamamoto, *Rev. Mod. Phys.* **82**, 1489 (2010).
- [3] A. Amo, J. Lefrère, S. Pigeon, C. Adrados, C. Ciuti, I. Carusotto, R. Houdré, E. Giacobino, and A. Bramati, *Nature Physics* **5**, 805 EP (2009).
- [4] V. Kohnle, Y. Léger, M. Wouters, M. Richard, M. T. Portella-Oberli, and B. Deveaud-Plédran, *Phys. Rev. Lett.* **106**, 255302 (2011).
- [5] K. G. Lagoudakis, M. Wouters, M. Richard, A. Baas, I. Carusotto, R. André, L. S. Dang, and B. Deveaud-Plédran, *Nature Physics* **4**, 706 (2008).
- [6] T. Ozawa, H. M. Price, A. Amo, N. Goldman, M. Hafezi, L. Lu, M. C. Rechtsman, D. Schuster, J. Simon, O. Zeitler, and I. Carusotto, *Rev. Mod. Phys.* **91**, 015006 (2019).
- [7] T. Karzig, C.-E. Bardyn, N. H. Lindner, and G. Refael, *Phys. Rev. X* **5**, 031001 (2015).
- [8] P. St-Jean, V. Goblot, E. Galopin, A. Lemaître, T. Ozawa, L. Le Gratiet, I. Sagnes, J. Bloch, and A. Amo, *Nature Photonics* **11**, 651 (2017).
- [9] S. Klemmt, T. H. Harder, O. A. Egorov, K. Winkler, R. Ge, M. A. Bandres, M. Emmerling, L. Worschech, T. C. H. Liew, M. Segev, C. Schneider, and S. Höfling, *Nature* **562**, 552 (2018).
- [10] M. Sidler, P. Back, O. Cotlet, A. Srivastava, T. Fink, M. Kroner, E. Demler, and A. Imamoglu, *Nature Physics* **13**, 255 EP (2016).
- [11] D. K. Efimkin, E. K. Laird, J. Levinsen, M. M. Parish, and A. H. MacDonald, *Phys. Rev. B* **103**, 075417 (2021).
- [12] M. A. Bastarrachea-Magnani, A. Camacho-Guardian, and G. M. Bruun, “Attractive and repulsive exciton-polariton interactions mediated by an electron gas,” (2020), [arXiv:2008.10303 \[cond-mat.mes-hall\]](https://arxiv.org/abs/2008.10303).
- [13] L. B. Tan, O. Cotlet, A. Bergschneider, R. Schmidt, P. Back, Y. Shimazaki, M. Kroner, and A. m. c. Imamoglu, *Phys. Rev. X* **10**, 021011 (2020).
- [14] R. P. A. Emmanuele, M. Sich, O. Kyriienko, V. Shahnazaryan, F. Withers, A. Catanzaro, P. M. Walker, F. A. Benimetskiy, M. S. Skolnick, A. I. Tartakovskii, I. A. Shelykh, and D. N. Krizhanovskii, *Nature Communications* **11**, 3589 (2020).
- [15] J. R. Schaibley, H. Yu, G. Clark, P. Rivera, J. S. Ross, K. L. Seyler, W. Yao, and X. Xu, *Nature Reviews Materials* **1**, 16055 EP (2016), review Article.
- [16] G. Wang, A. Chernikov, M. M. Glazov, T. F. Heinz, X. Marie, T. Amand, and B. Urbaszek, *Rev. Mod. Phys.* **90**, 021001 (2018).
- [17] D. K. Efimkin and A. H. MacDonald, *Phys. Rev. B* **97**, 235432 (2018).
- [18] Y.-C. Chang, S.-Y. Shiau, and M. Combescot, *Phys. Rev. B* **98**, 235203 (2018).
- [19] We skip the *exciton* label for brevity.
- [20] R. Rapaport, E. Cohen, A. Ron, E. Linder, and L. N. Pfeiffer, *Phys. Rev. B* **63**, 235310 (2001).
- [21] D. K. Efimkin and A. H. MacDonald, *Phys. Rev. B* **95**, 035417 (2017).
- [22] O. Kyriienko, D. N. Krizhanovskii, and I. A. Shelykh, *Phys. Rev. Lett.* **125**, 197402 (2020).
- [23] M. M. Glazov, *The Journal of Chemical Physics* **153**, 034703 (2020), <https://doi.org/10.1063/5.0012475>.
- [24] F. Rana, O. Koksai, and C. Manolatu, *Phys. Rev. B* **102**, 085304 (2020).
- [25] O. Cotlet, S. Zeytinoglu, M. Sigrist, E. Demler, and A. m. c. Imamoglu, *Phys. Rev. B* **93**, 054510 (2016).
- [26] B. J. DeSalvo, K. Patel, G. Cai, and C. Chin, *Nature* **568**, 61 (2019).
- [27] R. S. Lous, I. Fritsche, M. Jag, F. Lehmann, E. Kirilov, B. Huang, and R. Grimm, *Phys. Rev. Lett.* **120**, 243403 (2018).
- [28] I. Ferrier-Barbut, M. Delehaye, S. Laurent, A. T. Grier, M. Pierce, B. S. Rem, F. Chevy, and C. Salomon, *Science* **345**, 1035 (2014), <https://science.sciencemag.org/content/345/6200/1035.full.pdf>.
- [29] I. Fritsche, C. Baroni, E. Dobler, E. Kirilov, B. Huang, R. Grimm, G. M. Bruun, and P. Massignan, “Stability and breakdown of fermi polarons in a strongly interacting fermi-bose mixture,” (2021), [arXiv:2103.03625 \[cond-mat.quant-gas\]](https://arxiv.org/abs/2103.03625).
- [30] O. Bleu, G. Li, J. Levinsen, and M. M. Parish, *Phys. Rev. Research* **2**, 043185 (2020).
- [31] J. J. Hopfield, *Phys. Rev.* **112**, 1555 (1958).
- [32] P. Massignan, M. Zaccanti, and G. M. Bruun, *Reports on Progress in Physics* **77**, 034401 (2014).
- [33] See *Supplemental Material* online for details on the strong coupling theory for polaron-polaritons, the non-equilibrium theory for the condensate and the origin of non-linear features of Fig. 1(c), which includes Refs. [58–62].
- [34] M. A. Bastarrachea-Magnani, A. Camacho-Guardian, M. Wouters, and G. M. Bruun, *Phys. Rev. B* **100**, 195301 (2019).
- [35] M. Wouters, *Phys. Rev. B* **76**, 045319 (2007).
- [36] I. Carusotto, T. Volz, and A. Imamoglu, *EPL (Europhysics Letters)* **90**, 37001 (2010).
- [37] K. F. Mak, K. He, C. Lee, G. H. Lee, J. Hone, T. F. Heinz, and J. Shan, *Nature Materials* **12**, 207 EP (2012).
- [38] G. F. Giuliani and G. Vignale, *Quantum Theory of the Electron Liquid* (Cambridge University Press, 2005).
- [39] A. Camacho-Guardian and G. M. Bruun, *Phys. Rev. X* **8**, 031042 (2018).
- [40] C. Ciuti, V. Savona, C. Piermarocchi, A. Quattropani, and P. Schwendimann, *Phys. Rev. B* **58**, 7926 (1998).
- [41] L. Ferrier, E. Wertz, R. Johne, D. D. Solnyshkov, P. Senellart, I. Sagnes, A. Lemaître, G. Malpuech, and J. Bloch, *Phys. Rev. Lett.* **106**, 126401 (2011).
- [42] S. R. K. Rodriguez, A. Amo, I. Sagnes, L. Le Gratiet, E. Galopin, A. Lemaître, and J. Bloch, *Nature Communications* **7**, 11887 EP (2016), article.
- [43] A. Delteil, T. Fink, A. Schade, S. Höfling, C. Schneider,

- and A. Amo, *Nature Materials* **18**, 219 (2019).
- [44] V. Shahnazaryan, I. Iorsh, I. A. Shelykh, and O. Kyriienko, *Phys. Rev. B* **96**, 115409 (2017).
- [45] F. Barachati, A. Fieramosca, S. Hafezian, J. Gu, B. Chakraborty, D. Ballarini, L. Martinu, V. Menon, D. Sanvitto, and S. Kéna-Cohen, *Nature Nanotechnology* **13**, 906 (2018).
- [46] I. Carusotto and C. Ciuti, *Phys. Rev. Lett.* **93**, 166401 (2004).
- [47] C. Ciuti and I. Carusotto, *physica status solidi (b)* **242**, 2224 (2005).
- [48] I. Carusotto and C. Ciuti, *Rev. Mod. Phys.* **85**, 299 (2013).
- [49] A. Baas, J. P. Karr, H. Eleuch, and E. Giacobino, *Phys. Rev. A* **69**, 023809 (2004).
- [50] D. Ballarini, M. De Giorgi, E. Cancellieri, R. Houdr , E. Giacobino, R. Cingolani, A. Bramati, G. Gigli, and D. Sanvitto, *Nature Communications* **4**, 1778 (2013).
- [51] D. Bajoni, M. Perrin, P. Senellart, A. Lemaître, B. Sermage, and J. Bloch, *Phys. Rev. B* **73**, 205344 (2006).
- [52] A. Camacho-Guardian, M. Bastarrachea-Magnani, and G. M. Bruun, “Mediated interactions and photon bound states in an exciton-polariton mixture,” (2020), [arXiv:2003.04659](https://arxiv.org/abs/2003.04659) [cond-mat.mes-hall].
- [53] E. Fratini and P. Pieri, *Phys. Rev. A* **88**, 013627 (2013).
- [54] A. Guidini, G. Bertaina, D. E. Galli, and P. Pieri, *Phys. Rev. A* **91**, 023603 (2015).
- [55] Z. Wu and G. M. Bruun, *Phys. Rev. Lett.* **117**, 245302 (2016).
- [56] T. Ozawa, A. Recati, M. Delehay , F. Chevy, and S. Stringari, *Phys. Rev. A* **90**, 043608 (2014).
- [57] C. Lobo, A. Recati, S. Giorgini, and S. Stringari, *Phys. Rev. Lett.* **97**, 200403 (2006).
- [58] A. Fetter and J. Walecka, *Quantum Theory of Many-Particle Systems*, Dover Books on Physics Series (Dover Publications, 1971).
- [59] M. Randeria, J.-M. Duan, and L.-Y. Shieh, *Phys. Rev. B* **41**, 327 (1990).
- [60] R. Schmidt, T. Enss, V. Pietil , and E. Demler, *Phys. Rev. A* **85**, 021602 (2012).
- [61] P. Meystre and M. Sargent III, *Elements of Quantum Optics* (Springer-Verlag, 2007).
- [62] M. Scully and M. Zubairy, *Quantum Optics* (Cambridge University Press, 1997).

# Bose-Einstein condensation of exciton polaron-polaritons: supplementary material

Aleksi Julku,<sup>1</sup> Miguel. A. Bastarrachea-Magnani,<sup>1,2</sup> Arturo Camacho-Guardian,<sup>3</sup> and Georg Bruun<sup>1,4</sup>

<sup>1</sup>*Department of Physics and Astronomy, Aarhus University, Ny Munkegade, DK-8000 Aarhus C, Denmark*

<sup>2</sup>*Departamento de Física, Universidad Autónoma Metropolitana-Iztapalapa, San Rafael Atlixco 186, C. P. 09340, Ciudad de México, México*

<sup>3</sup>*T.C.M. Group, Cavendish Laboratory, University of Cambridge, JJ Thomson Avenue, Cambridge, CB3 0HE, U.K*

<sup>4</sup>*Shenzhen Institute for Quantum Science and Engineering and Department of Physics, Southern University of Science and Technology, Shenzhen 518055, China*

(Dated: February 11, 2022)

## EXCITON-EXCITON INTERACTIONS

The interaction Hamiltonian between electrons and excitons is

$$H_{int} = \sum_{\mathbf{k}, \mathbf{k}', \mathbf{q}} g_{ex} \hat{x}_{\mathbf{k}' - \mathbf{q}}^\dagger \hat{e}_{\mathbf{k} + \mathbf{q}}^\dagger \hat{e}_{\mathbf{k}} \hat{x}_{\mathbf{k}'}. \quad (1)$$

We base our approach on the Bethe-Salpeter equation considering the repeated forward scattering between an exciton and an electron as illustrated in Fig. 1(a). This so-called ladder approximation yields the  $\mathcal{T}$ -matrix [1, 2]:

$$\mathcal{T}(\mathbf{k}, i\omega_n) = g_{ex} + g_{ex} \Pi(\mathbf{k}, i\omega_n) \mathcal{T}(\mathbf{k}, i\omega_n) \Leftrightarrow \mathcal{T}^{-1}(\mathbf{k}, i\omega_n) = g_{ex}^{-1} - \Pi(\mathbf{k}, i\omega_n), \quad (2)$$

where  $\omega_n = \frac{(2n+1)\pi}{\beta}$  are fermionic Matsubara frequencies ( $n$  is an integer,  $\beta = \frac{1}{k_B T}$ ,  $k_B$  is the Boltzmann constant and  $T$  is the temperature) and the exciton-electron pair-propagator  $\Pi(\mathbf{k}, i\omega_n)$  reads

$$\Pi(\mathbf{k}, i\omega_n) = -\frac{1}{\beta} \int \frac{d^2 \mathbf{q}}{(2\pi)^2} \sum_{iq_n} G_x^0(\mathbf{k} + \mathbf{q}, iq_n) G_e^0(-\mathbf{q}, i\omega_n - iq_n). \quad (3)$$

Here  $q_n = \frac{2\pi n}{\beta}$  are bosonic Matsubara frequencies and the non-interacting Green's functions for the excitons and electrons are,  $G_x^0(\mathbf{k}, z) = 1/(z - \epsilon_{x\mathbf{k}} + \mu_x)$  and  $G_e^0(\mathbf{k}, z) = 1/(z - \epsilon_{e\mathbf{k}} + \mu_e)$ , respectively, with excitonic and electronic chemical potentials  $\mu_x$  and  $\mu_e$ .

In the limit of a single exciton-impurity, the pair propagator is

$$\Pi(\mathbf{k}, i\omega_n) = \int \frac{d^2 \mathbf{q}}{(2\pi)^2} \frac{1 - n_F(\epsilon_{e\mathbf{k}} - \mu_e)}{i\omega_n - \epsilon_{e\mathbf{q}} - \epsilon_{x\mathbf{k} + \mathbf{q}} + \mu_e}. \quad (4)$$

We use this form in the calculations as we are interested in the energy spectrum of a single polaron-polariton.

In the vacuum limit, i.e. when a single exciton scatters with a single electron, the Bethe-Salpeter is an exact solution of the two-body problem. In this case, the two-body  $\mathcal{T}$ -matrix can be written as  $\mathcal{T}_V^{-1}(0, i\omega_n) = g_{ex}^{-1} - \Pi_V(0, i\omega_n)$ . In a two-dimensional system the two-body scattering problem always features a bound state of energy  $-\epsilon_B < 0$  [3] which manifests as a pole of  $\mathcal{T}_V$  such that  $g_{ex}^{-1} = \text{Re}[\Pi_V(0, -\epsilon_B)]$ . In case of the exciton-polaron problem, this bound state corresponds to the trion [4–7]. The many-body  $\mathcal{T}$ -matrix can then be recast in the renormalized form as

$$\mathcal{T}^{-1}(\mathbf{k}, i\omega_n) = \text{Re}[\Pi_V(0, -\epsilon_B)] - \Pi(\mathbf{k}, i\omega_n). \quad (5)$$

The vacuum pair-propagator  $\Pi_V$  reads

$$\Pi_V(0, -\epsilon_B) = -\frac{m_e}{2\pi(1 + \alpha)} \log \left[ \frac{(1 + \alpha)\Lambda^2}{2m_e \epsilon_B} \right], \quad (6)$$

where  $\Lambda$  is the ultraviolet momentum cut-off and  $\alpha = m_e/m_x$ . With large enough  $\Lambda$ , the ultraviolet divergences of  $\Pi_V$  and  $\Pi$  cancel each other and  $\mathcal{T}$  is a well-defined function independent of  $\Lambda$ .

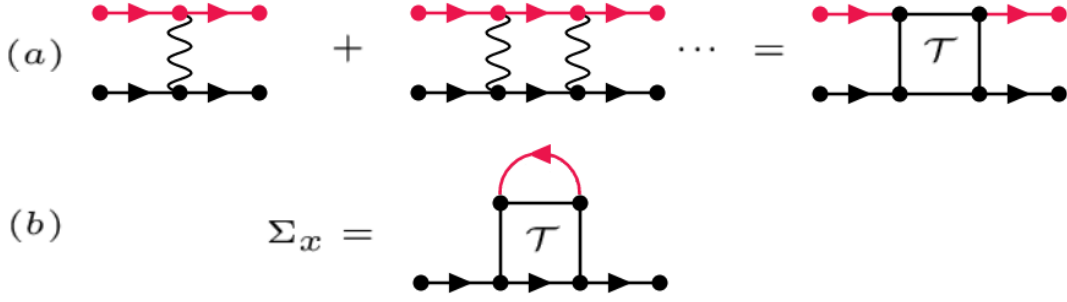


FIG. 1. (a) Ladder approximation and the  $\mathcal{T}$ -matrix. Solid black (red) lines correspond to exciton (electron) propagators and wavy lines represent bare exciton-electron interaction vertices  $g_{ex}$  (b) Exciton self-energy  $\Sigma_x$ .

We employ a diagrammatic approach based on the  $\mathcal{T}$ -matrix, that takes into account the underlying trion-state. The self-energy for the excitons  $\Sigma_x(\mathbf{k}, i\omega_n)$  within the  $\mathcal{T}$ -matrix approximation is depicted in Fig.1(b), and given explicitly by

$$\Sigma_x(\mathbf{k}, i\omega_n) = \frac{1}{\beta} \int \frac{d^2\mathbf{q}}{(2\pi)^2} \sum_{iq_n} G_e^0(\mathbf{q}, iq_n) \mathcal{T}(\mathbf{k} + \mathbf{q}, i\omega_n + iq_n). \quad (7)$$

Here  $i\omega_n$  are now bosonic Matsubara frequencies. As we are considering the single exciton-impurity limit,  $\Sigma_x$  simply reads

$$\Sigma_x(\mathbf{k}, i\omega_n) = \int \frac{d^2\mathbf{q}}{(2\pi)^2} n_F(\epsilon_{e\mathbf{q}} - \mu_e) \mathcal{T}(\mathbf{k} + \mathbf{q}, i\omega_n + \epsilon_{e\mathbf{q}} - \mu_e). \quad (8)$$

The full Green's function for excitons is then  $G_x^{-1}(\mathbf{k}, i\omega_n) = z - \epsilon_{x\mathbf{k}} - \Sigma_x(\mathbf{k}, i\omega_n)$ . By computing the energy poles of  $G_x$ , one finds that  $\Sigma_x$  gives rise to the attractive and repulsive Fermi-polaron states in the absence of light [7], in a similar fashion as in Fermi gases [8, 9]. The cavity photon field then couples to the polaron states giving rise to three exciton polaron-polariton branches as it is shown in Fig. 2(a) of the main text.

The emergence of exciton polaron-polaritons can be studied with the  $2 \times 2$  Green's function describing both excitonic and photonic degrees of freedom. More precisely, we define  $G(\mathbf{k}, \tau) = -\langle T_\tau \{ \hat{\Psi}_{\mathbf{k}}(\tau) \hat{\Psi}_{\mathbf{k}}^\dagger(0) \} \rangle$ , where  $\hat{\Psi}_{\mathbf{k}}^\dagger \equiv [\hat{x}_{\mathbf{k}}^\dagger \ \hat{c}_{\mathbf{k}}^\dagger]$  and  $T_\tau$  is the imaginary time-ordering operator. In the frequency space, we have [7]

$$G^{-1}(\mathbf{k}, ik_n) = \begin{bmatrix} ik_n - \epsilon_{x\mathbf{k}} - \Sigma_x(\mathbf{k}, ik_n) & -\Omega \\ -\Omega & ik_n - \epsilon_{c\mathbf{k}} \end{bmatrix}, \quad (9)$$

which is the form used in the main text.

## NON-EQUILIBRIUM BOSE CONDENSATION AND BOGOLIUBOV THEORY

In this section, we provide details on the derivation of the non-equilibrium Gross-Pitaevskii equation (GPE) and the Bogoliubov equations giving the excitation spectrum. To treat the incoherent decay terms of polaritons correctly, we deploy a formalism where the bosonic polariton modes are coupled to an external thermal reservoir bath of harmonic oscillators [10, 11]. The role of the reservoir is to take into account the open quantum system nature of the polaron-polariton setup. By assuming that the correlation times of the bath are much smaller than any relevant time scale of the polariton system, i.e. by employing a Markovian approximation, one ends up with the equations of motion which describe the decay of the polaritons.

We emphasize that the right form for the non-equilibrium Green's function can not be obtained with a non-hermitian decay Hamiltonian of the form  $H_{decay} = \sum_{\mathbf{k}} i\gamma \hat{b}_{\mathbf{k}}^\dagger \hat{b}_{\mathbf{k}}$ , where  $\hat{b}_{\mathbf{k}}$  are the annihilation operators for the polaron-polariton state at  $\mathbf{k}$ . This can be seen from the Heisenberg equation of motion which yields  $\frac{d\hat{b}_{\mathbf{k}}}{dt} = -i[\hat{b}_{\mathbf{k}}, H_{decay}] = -i\gamma \hat{b}_{\mathbf{k}}$  but  $\frac{d\hat{b}_{\mathbf{k}}^\dagger}{dt} = i\gamma \hat{b}_{\mathbf{k}}^\dagger$ . The solutions for these differential equations give a damping solution for  $\hat{b}_{\mathbf{k}}$  but an unphysical amplifying solution for  $\hat{b}_{\mathbf{k}}^\dagger$ . This inevitably leads to a wrong non-equilibrium theory. Below, we derive the Bogoliubov theory accounting correctly for the losses of the polaron-polaritons, preventing unphysical amplifications of the bosonic fields.

We start by writing down the effective Hamiltonian for the lower polaron-polaritons in the presence an external coherent driving field and incoherent losses:

$$\begin{aligned}
H_L &= H_s + H_r + H_{sr}, \text{ where} \\
H_s &= \sum_{\mathbf{k}} \epsilon_{\mathbf{k}}^L \hat{b}_{\mathbf{k}}^\dagger \hat{b}_{\mathbf{k}} + \frac{g}{2V} \sum_{\mathbf{k}, \mathbf{k}', \mathbf{q}} \hat{b}_{\mathbf{k}}^\dagger \hat{b}_{\mathbf{k}'}^\dagger \hat{b}_{\mathbf{k}'-\mathbf{q}} \hat{b}_{\mathbf{k}+\mathbf{q}} + iE_{\text{pu}} e^{-i\epsilon_{\text{pu}} t} \hat{b}_{\mathbf{k}_{\text{pu}}}^\dagger, \\
H_r &= \sum_j \epsilon_j^B \hat{r}_j^\dagger \hat{r}_j \\
H_{sr} &= \sum_{\mathbf{k}, j} [\kappa_j^* \hat{b}_{\mathbf{k}}^\dagger \hat{r}_j + \kappa_j \hat{r}_j^\dagger \hat{b}_{\mathbf{k}}].
\end{aligned} \tag{10}$$

Here the polaron-polaritons are described by the system Hamiltonian  $H_s$ , the reservoir bath is  $H_r$  and the coupling between the system and the bath is treated via  $H_{sr}$ . The polaron-polariton energies are denoted by  $\epsilon_{\mathbf{k}}^L$ ,  $V$  is the system volume,  $g$  is the effective interaction between polaron-polaritons,  $E_{\text{pu}}$  is the strength of the laser pump,  $\epsilon_{\text{pu}}$  is the pump energy and  $\mathbf{k}_{\text{pu}}$  is the in-plane momentum of the pump ( $\hbar = 1$ ). In  $H_r$ ,  $\hat{r}_j$  are the annihilation operators for the  $j$ th reservoir mode of energy  $\epsilon_j^B$ . In  $H_{sr}$  we have employed the Rotating Wave Approximation (RWA) by assuming that the bandwidth of the bath is much larger than the system-reservoir coupling  $\kappa_j$  such that the non-energy-conserving terms have been discarded in  $H_{sr}$ .

By writing down the Heisenberg equation of motions for  $\hat{b}_{\mathbf{k}}$  and  $\hat{r}_j$ , and deploying the Markovian approximation for the system-reservoir coupling [10, 11], we obtain, after a straightforward algebra, the following

$$i \frac{\partial \hat{b}_{\mathbf{k}}}{\partial t} = (\epsilon_{\mathbf{k}}^L - i\gamma) \hat{b}_{\mathbf{k}} + iE_{\text{pu}} e^{-i\epsilon_{\text{pu}} t} \delta_{\mathbf{k}, \mathbf{k}_{\text{pu}}} + [\hat{b}_{\mathbf{k}}, \frac{g}{2V} \sum_{\mathbf{k}, \mathbf{k}', \mathbf{q}} \hat{b}_{\mathbf{k}}^\dagger \hat{b}_{\mathbf{k}'}^\dagger \hat{b}_{\mathbf{k}'-\mathbf{q}} \hat{b}_{\mathbf{k}+\mathbf{q}}], \tag{11}$$

where the polaron-polariton decay is  $\gamma = 2\pi |\kappa(\epsilon_{\mathbf{k}}^L)|^2 \mathcal{D}(\epsilon_{\mathbf{k}}^L)$  with  $\kappa(\epsilon)$  being a continuous interpolation of  $\kappa_j$  and  $\mathcal{D}(\epsilon)$  the density of the states of the reservoir [11]. The microscopic details of the reservoir are not important and thus for  $\gamma$  we pick an experimentally realistic value of  $\gamma = 0.4$  meV. Moreover, we have ignored for simplicity the quantum noise term arising from the system-reservoir coupling.

For the purpose of this work, we choose  $\mathbf{k}_{\text{pu}} = 0$ . Now we assume that the polaron-polariton state at  $\mathbf{k}_{\text{pu}}$  goes through a Bose condensation and thus acquires a macroscopic population due to the pump. We therefore approximate  $\hat{b}_{\mathbf{k}_{\text{pu}}}$  as a complex number such that  $\hat{b}_{\mathbf{k}_{\text{pu}}} \approx \sqrt{V} \Psi_0(t)$ , where  $\Psi_0(t)$  is the condensation wave function. At the Gross-Pitaevskii mean-field level, the contribution of states of  $\mathbf{k} \neq \mathbf{k}_{\text{pu}}$  is neglected and from Eq. (11) we obtain for the condensed state the following:

$$i\partial \Psi_0(t) = (\epsilon_0 - i\gamma) \Psi_0(t) + iE_{\text{pu}} e^{-i\epsilon_{\text{pu}} t} + g |\Psi_0(t)|^2 \Psi_0(t), \tag{12}$$

where  $\epsilon_0 \equiv \epsilon_{\mathbf{k}=0}^L$ . By assuming that the condensate wave function follows the time dependence of the driving field, i.e.  $\Psi_0(t) = \Psi_0 e^{-i\epsilon_{\text{pu}} t}$ , one acquires the non-equilibrium Gross-Pitaevskii equation:

$$\epsilon_{\text{pu}} \Psi_0 = (\epsilon_0 - i\gamma) \Psi_0 + iE_{\text{pu}} + g |\Psi_0|^2 \Psi_0, \tag{13}$$

which is the same as Eq. (6) in the main text.

The condensation wave function can be written as  $\Psi_0 = \sqrt{n_0} e^{i\phi_0}$ , where  $n_0$  is the condensation density. In case of an equilibrium condensate, any value of  $\phi_0$  would yield the same ground state energy and equally well provide a solution for the equilibrium GPE. However, it turns out that the non-equilibrium GPE of Eq. (13) can be solved in general only for some specific value of  $\phi_0$ , i.e. the external pumping breaks explicitly the  $U(1)$  phase symmetry by picking a definite complex phase  $\phi_0$  for the condensation wave function.

Now we study the excitation spectrum of the non-equilibrium BEC. To this end, we write  $\hat{b}_{\mathbf{k}}$  as

$$\hat{b}_{\mathbf{k}} = [\sqrt{V} \Psi_0 \delta_{\mathbf{k}, 0} + \delta \hat{b}_{\mathbf{k}}(t)] e^{-i\epsilon_{\text{pu}} t}, \tag{14}$$

where we have introduced the fluctuation term on top of the condensate,  $\delta \hat{b}_{\mathbf{k}}(t)$ , to account for the non-condensed polaron-polaritons. To describe the fluctuations, we introduce the bosonic Green's function which in the imaginary-time domain reads

$$G_B(\mathbf{k}, \tau) \equiv -\langle T_\tau \begin{bmatrix} \delta \hat{b}_{\mathbf{k}}(\tau) \\ \delta \hat{b}_{-\mathbf{k}}^\dagger(\tau) \end{bmatrix} [\delta \hat{b}_{\mathbf{k}}^\dagger(0) \quad \delta \hat{b}_{-\mathbf{k}}(0)] \rangle = \begin{bmatrix} -\langle T_\tau \delta \hat{b}_{\mathbf{k}}(\tau) \delta \hat{b}_{\mathbf{k}}^\dagger(0) \rangle & -\langle T_\tau \delta \hat{b}_{\mathbf{k}}(\tau) \delta \hat{b}_{-\mathbf{k}}(0) \rangle \\ -\langle T_\tau \delta \hat{b}_{-\mathbf{k}}^\dagger(\tau) \delta \hat{b}_{\mathbf{k}}^\dagger(0) \rangle & -\langle T_\tau \delta \hat{b}_{-\mathbf{k}}^\dagger(\tau) \delta \hat{b}_{-\mathbf{k}}(0) \rangle \end{bmatrix}, \tag{15}$$

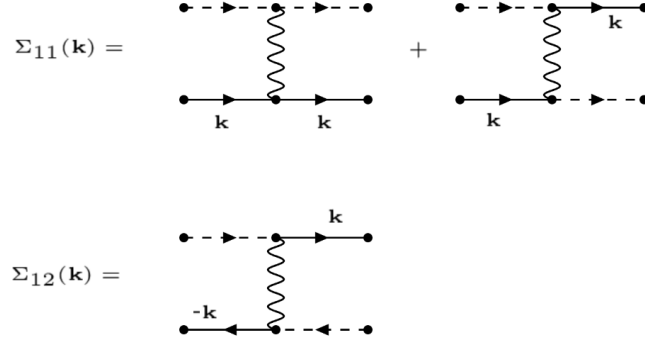


FIG. 2. Self-energy diagrams included in the Bogoliubov approximation. The solid propagators are the non-condensed polaron-polaritons, whereas the dashed lines depict polariton-polaritons propagating into and out of the condensate with the wavefunction  $\Psi = \sqrt{n_0}e^{i\phi_0}$ . The wavy lines depict the interaction polariton interaction  $g$ .

where  $\mathbf{k} \neq 0$  as we are considering the non-condensed polaron-polaritons only. In the Matsubara frequency space one has the Dyson equation [1]:

$$G_B^{-1}(\mathbf{k}, i\omega_n) = G_{B,0}^{-1}(\mathbf{k}, i\omega_n) - \Sigma_B(\mathbf{k}, i\omega_n). \quad (16)$$

Here  $\Sigma_B$  is the self-energy arising from finite interactions between polariton-polaritons and  $G_{B,0}$  is the non-interacting Green's function, i.e. in the absence of interactions,  $g = 0$ , one has  $G_B = G_{B,0}$ .

To proceed, we first evaluate  $G_{B,0}$ . We denote the Hamiltonian without the interactions as  $H_0 \equiv H_L(g = 0)$ . Then, by using the Markovian approximation and ignoring the quantum noise terms, we obtain the following imaginary-time equations of motion [10, 11]:

$$\begin{aligned} [\delta\hat{b}_{\mathbf{k}}(\tau)e^{\epsilon_{\text{pu}}\tau}, H_0] &= (-\epsilon_{\mathbf{k}}^L + i\gamma)\delta\hat{b}_{\mathbf{k}}(\tau)e^{\epsilon_{\text{pu}}\tau} \\ [\delta\hat{b}_{\mathbf{k}}^\dagger(\tau)e^{-\epsilon_{\text{pu}}\tau}, H_0] &= (\epsilon_{\mathbf{k}}^L + i\gamma)\delta\hat{b}_{\mathbf{k}}^\dagger(\tau)e^{-\epsilon_{\text{pu}}\tau}. \end{aligned} \quad (17)$$

The latter equation would have a wrong form for the decay part if we had used the non-hermitian form  $H_{decay} = \sum_{\mathbf{k}} i\gamma\hat{b}_{\mathbf{k}}^\dagger\hat{b}_{\mathbf{k}}$  describing the decay instead of the system-reservoir formalism. Now, it is straightforward to take the time derivative of  $G_{B,0}(\mathbf{k}, \tau)$  to show that

$$\begin{aligned} \partial_\tau[G_{B,0}(\mathbf{k}, \tau)]_{11} &= -\delta(\tau) - (\epsilon_{\mathbf{k}}^L - i\gamma - \epsilon_{\text{pu}})[G_{B,0}(\mathbf{k}, \tau)]_{11} \\ \partial_\tau[G_{B,0}(\mathbf{k}, \tau)]_{22} &= \delta(\tau) + (\epsilon_{\mathbf{k}}^L + i\gamma - \epsilon_{\text{pu}})[G_{B,0}(\mathbf{k}, \tau)]_{22}. \end{aligned} \quad (18)$$

By transforming these expressions to the Matsubara frequency space, one has

$$G_{B,0}^{-1}(\mathbf{k}, z) = \begin{bmatrix} z - \tilde{\epsilon}_{\mathbf{k}} + i\gamma & 0 \\ 0 & -z - \tilde{\epsilon}_{\mathbf{k}} - i\gamma \end{bmatrix}, \quad (19)$$

where  $\tilde{\epsilon}_{\mathbf{k}} \equiv \epsilon_{\mathbf{k}}^L - \epsilon_{\text{pu}}$ .

The self-energy  $\Sigma_B$  can be in general evaluated with the diagrammatic Beliaev theory [1]. Here, we deploy the first order Beliaev theory, i.e. the Bogoliubov theory that includes only the diagrams presented in Fig. 2. Since we are interested on low-energy states, for simplicity for the scattering between two polaritons with momenta  $\mathbf{k}$  and  $\mathbf{k}'$  that exchange a momentum  $\mathbf{q}$  we approximate the polariton-polariton interactions by  $g_{\mathbf{k}, \mathbf{k}'; \mathbf{q}} = g = g_{xx}\tilde{C}(\mathbf{k} = 0)^4 Z^2(\mathbf{k} = 0)$ , and based on the same argument, we assume a momentum independent damping rate  $\gamma$ . Then the Bogoliubov self-energy reads as follows,

$$\Sigma_B = \begin{bmatrix} 2gn_0 & gn_0e^{i2\phi_0} \\ gn_0e^{-i2\phi_0} & 2gn_0 \end{bmatrix}. \quad (20)$$

By inserting the expressions (19) and (20) to the Dyson equation of Eq. (16), one finally obtains the Bogoliubov Green's function used in the main text:

$$G_B^{-1}(\mathbf{k}, z) = \begin{bmatrix} z - \tilde{\epsilon}_{\mathbf{k}} + i\gamma - 2gn_0 & -gn_0e^{i2\phi_0} \\ -gn_0e^{-i2\phi_0} & -z - \tilde{\epsilon}_{\mathbf{k}} - i\gamma - 2gn_0 \end{bmatrix} \quad (21)$$

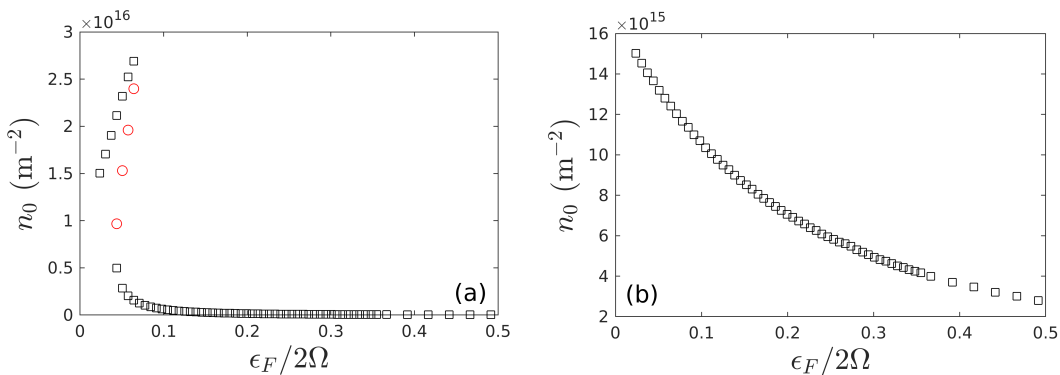


FIG. 3. (a) Condensate density  $n_0$  as a function of electron density for fixed  $g(\epsilon_F/2\Omega = 0.023)/g_{xx} = 0.0029$ . (b) Condensate density  $n_0$  as a function of electron density for fixed  $\epsilon_0(\epsilon_F/2\Omega = 0.023)/2\Omega = -2.224$ . Black square (red dots) indicate stable (unstable) solutions for the non-equilibrium GPE. The pump intensity and energy are the same as in Figs.1(b)-(c) of the main text.

Excitation spectrum is then given by  $\det[G_B^{-1}(\mathbf{k}, E_{\mathbf{k}})] = 0$ , yielding the dispersion relation written down in the main text. As the complex phase of condensation wave function,  $\phi_0$ , does not affect the excitation spectrum or the stability condition,  $\text{Im}[E_{\mathbf{k}}] < 0$ , we have in the main text for simplicity set  $\phi_0 = 0$  in the expression of  $G_B^{-1}(\mathbf{k}, z)$ .

### ORIGIN OF NON-LINEAR FEATURES

In this section we point out the origin of two different non-linear regimes seen in the low- and high- $\epsilon_F$  limits presented in Fig. 1(c) of the main text. We specifically show that the non-linear feature in the low- $\epsilon_F$  regime arises predominantly from the increasing blue detuning of the laser, i.e.  $\epsilon_{\text{pu}} - \epsilon_0$ , as a function of increasing  $\epsilon_F$ , whereas the high- $\epsilon_F$  non-linear feature results in from the interplay of both increasing  $\epsilon_{\text{pu}} - \epsilon_0$  and  $g$  as a function of the electron density.

To demonstrate these claims, we performed two computations: one with fixed  $\epsilon_0$  and one with fixed  $g$  such that in both the computations either only  $\epsilon_0$  or  $g$  was allowed to change as a function of  $\epsilon_F$ . The results are shown in Fig. 3: in Fig. 3(a) we show  $n_0$  as a function of  $\epsilon_F$  by fixing the interaction  $g$ , whereas in Fig. 3(b) the polaron-polariton ground state energy  $\epsilon_0$  is held fixed. The pump intensity and frequency are the same as in Fig. 1(c) of the main text. In Fig. 3(a) [Fig. 3(b)] the value of interaction  $g$  (ground state energy  $\epsilon_0$ ) is given by the lowest value of  $\epsilon_F$ , i.e.  $g/g_{xx} = 0.0029$  ( $\epsilon_0/2\Omega = 0.023$ ).

From Fig. 3(a) one observes that despite having a constant value for  $g$ , a non-linear behavior of three solutions can still be produced at the low- $\epsilon_F$  regime, in a similar fashion as in Fig. 1(c) of the main text. In contrast, with fixed  $\epsilon_0$  this feature is absent, see Fig. 3(b). As a consequence, the non-linear behavior seen at the low- $\epsilon_F$  regime in Fig. 1(c) of the main text arises due to the modification of  $\epsilon_0$  as a function of  $\epsilon_F$ .

From Fig. 3(a) we also see that for fixed  $g$  one cannot obtain a non-linear behavior at larger  $\epsilon_F$ , in contrast to the feature seen in Fig. 1(c) of the main text. Furthermore, the non-linearity is also absent with fixed  $\epsilon_0$ , see Fig. 3(b). We can thus conclude that the non-linear behavior at the high- $\epsilon_F$  regime in Fig. 1(c) of the main text arises because both  $\epsilon_0$  and  $g$  depend strongly on the electron density. Thus, such a non-linear feature cannot be achieved by simply tuning the pump energy in the absence of the 2DEG.

- 
- [1] A. Fetter and J. Walecka, *Quantum Theory of Many-Particle Systems*, Dover Books on Physics Series (Dover Publications, 1971).
  - [2] M. A. Bastarrachea-Magnani, A. Camacho-Guardian, M. Wouters, and G. M. Bruun, *Phys. Rev. B* **100**, 195301 (2019).
  - [3] M. Randeria, J.-M. Duan, and L.-Y. Shieh, *Phys. Rev. B* **41**, 327 (1990).
  - [4] M. Sidler, P. Back, O. Cotlet, A. Srivastava, T. Fink, M. Kroner, E. Demler, and A. Imamoglu, *Nature Physics* **13**, 255 EP (2016).
  - [5] K. F. Mak, K. He, C. Lee, G. H. Lee, J. Hone, T. F. Heinz, and J. Shan, *Nature Materials* **12**, 207 EP (2012).

- [6] L. B. Tan, O. Cotlet, A. Bergschneider, R. Schmidt, P. Back, Y. Shimazaki, M. Kroner, and A. m. c. İmamoğlu, [Phys. Rev. X](#) **10**, 021011 (2020).
- [7] M. A. Bastarrachea-Magnani, A. Camacho-Guardian, and G. M. Bruun, “Attractive and repulsive exciton-polariton interactions mediated by an electron gas,” (2020), [arXiv:2008.10303 \[cond-mat.mes-hall\]](#).
- [8] P. Massignan, M. Zaccanti, and G. M. Bruun, [Reports on Progress in Physics](#) **77**, 034401 (2014).
- [9] R. Schmidt, T. Enss, V. Pietilä, and E. Demler, [Phys. Rev. A](#) **85**, 021602 (2012).
- [10] P. Meystre and M. Sargent III, *Elements of Quantum Optics* (Springer-Verlag, 2007).
- [11] M. Scully and M. Zubairy, *Quantum Optics* (Cambridge University Press, 1997).